arXiv:1702.08482v1 [hep-th] 27 Feb 2017

IPM/P-2017/007

Far-from-equilibrium initial conditions probed by a nonlocal operator

L. Shahkarami[a,d,1], **H. Ebrahim**[b,d,2], **M. Ali-Akbari**[c,3], **F. Charmchi**[e,4]

[a] *School of Physics, Damghan University, Damghan, 41167-36716, Iran*
[b] *Department of Physics, University of Tehran, North Karegar Ave., Tehran 14395-547, Iran*
[c] *Department of Physics, Shahid Beheshti University G.C., Evin, Tehran 19839, Iran*
[d] *School of Physics, Institute for Research in Fundamental Sciences (IPM), P.O.Box 19395-5531, Tehran, Iran*
[e] *School of Particles and Accelerators, Institute for Research in Fundamental Sciences (IPM), P.O.Box 19395-5531, Tehran, Iran*
[1] *l.shahkarami@du.ac.ir,* [2] *hebrahim@ut.ac.ir,* [3] *m_aliakbari@sbu.ac.ir,* [4] *charmchi@ipm.ir*

Abstract

Using the gauge/gravity duality, we investigate the evolution of a strongly-coupled plasma which is initially anisotropic and/or non-conformal, from the viewpoint of the two-point function of scalar gauge-invariant operators with large conformal dimension. Considering various functions for the initial anisotropy and scalar field, we conclude that the effect of the anisotropy on the evolution of the two-point function is considerably more than the effect of the scalar field. We also show that the ordering of the equilibration time of the equilibration time of one-point function of the scalar field and the correlation function between two points with a fixed separation can be reversed by changing the initial configuration of the plasma, when there are at least two sources for driving the system out of the equilibrium. In addition, we find the equilibration time of the two-point function to be linearly increasing with respect to the separation of the two points with a fixed slope, regardless of the initial configuration that we start with. Finally we observe that, for larger separations the geodesic connecting two points on the boundary crosses the event horizon after it has reached its final equilibrium value, meaning that the two-point function can probe behind the event horizon.

1 Introduction

Understanding the out-of-equilibrium dynamics of a strongly-coupled gauge theory has attracted much interest in the past decade. One motivation for this comes from the results obtained in the ultra-relativistic heavy ion collisions at the Brookhaven RHIC and CERN LHC. The experimental observations, such as the elliptic flow, indicate that the hot and dense medium, created at the early moments of the collisions, is more similar to a perfect fluid with a small entropy-normalized viscosity than a collection of the individual partons [1, 2]. This medium called Quark-Gluon Plasma (QGP) is a strongly-coupled deconfined phase of QCD which is highly out of equilibrium and takes a very short time of order 1 fm/c to reach a thermalized state [3]. A challenging and still unresolved question is how a strongly-coupled out-of-equilibrium gauge theory evolves towards its thermal equilibrium.

A powerful tool to study the dynamics of such systems is the gauge/gravity duality [4–7] which solves the previously intractable problems using the classical gravitational dynamics of the asymptotically anti-de Sitter spacetimes. Plenty of work has been done on the early-time dynamics and subsequent thermalization in the past decade using various holographic techniques [8–24]. In particular, one way for investigating the dynamics of strongly-coupled far-from-equilibrium systems proposed in [10,11,19] is to drive the field theory out of equilibrium by distorting the metric for a finite amount of time in such a way that an anisotropy is created between the longitudinal and transverse directions. By solving the Einstein equations using the elegant method of characteristic formulation, they were able to study the isotropization of the system. Another way for investigating the early-time dynamics of far-from-equilibrium systems is to start from an out-of-equilibrium plasma, in the absence of external sources,

and then allow it to evolve and eventually reach its thermal equilibrium [14, 16]. In this approach the boundary metric is flat and time-independent, and the energy density is conserved. If the initial state is anisotropic, the pressure in the longitudinal and transverse directions will evolve in time and hence we are able to study the isotropization process.

One can also add an operator to the field theory and observe the time evolution of its one-point function for studying the thermalization process. In [22] we followed the second approach considering an initially anisotropic geometry interacting with a massive scalar field. We supposed that the expectation value of the scalar field at equilibrium is zero. Computing the pressure anisotropy and expectation value of the scalar field as time proceeds, we were able to study the process of approaching the equilibrium. For our purposes in most of the calculations we employed a Gaussian profile with tractable parameters as the initial function for both the scalar field and anisotropy function. By changing the parameters, we concluded that depending on the configuration of the initial plasma, various ordering of relaxation times, i.e. isotropization, thermalization and equilibration times, are possible. As introduced in [22], by these three time-scales we mean the time at which longitudinal and transverse pressures become equal, the entropy production ends, and the expectation value of the scalar field reaches its equilibrium, respectively, within the numerical precision chosen.

Extended objects such as correlation function of two local gauge invariant operators, expectation values of Wilson loops and entanglement entropy are more sensible to the details of the thermalization process than local probes [25–32]. Providing an elegant geometric way to compute these observables, AdS/CFT gives an explanation for this statement; nonlocal probes penetrate deeper into the bulk, hence probe a wider range of energies in the boundary field theory. Our purpose in the present paper is to investigate the thermalization process by studying the time evolution of the correlation function between two operators inserted in two equal-time points in the field theory. This operator is dual to a bulk field, according to the AdS/CFT dictionary. We consider the solution obtained in [22] as an out-of-equilibrium background. Then, according to the AdS/CFT dictionary, to obtain the two-point function in the field theory, we compute the time evolution of the geodesic length connecting the two points where the local operators are inserted at the boundary. Changing the initial configuration of the system, we would be able to study the evolution of the two-point function for different time ordering of the relaxation time-scales.

In the next section, we briefly review the calculation of the evolving background metric. Interested readers are referred to [22] and the above-mentioned original papers of the characteristic formulation, for more details. We explain the strategy we use for the calculation of the geodesic length in section 3. Finally, in section 4 we present the results of the numerical calculations for the geodesic length in some graphs and discuss about the thermalization time of the two-point function in different situations.

2 Evolution of an anisotropic spacetime with an scalar field

This section is devoted to a short review of the problem solved in [22]. The metric ansatz for an anisotropic asymptotically AdS_5 spacetime in the generalized Eddington-Finkelstein coordinates can be written in the following form

$$ds_5^2 = 2drdv - A(v,r)dv^2 + \Sigma(v,r)^2\left(e^{-2B(v,r)}dx_L^2 + e^{B(v,r)}d\mathbf{x}_T^2\right). \tag{1}$$

This metic is translationally invariant in the spatial coordinates of the boundary which is located at $r \to \infty$. v is the time coordinate in the bulk and is the boundary time as $r \to \infty$. The function $B(v,r)$ introduces an anisotropy between the longitudinal (x_L) and transverse ($\mathbf{x}_T$) directions of the boundary. We study the Einestein's general relativity minimally coupled to a massive scalar field with $m^2 = -3$ which is dual to a fermionic mass operator of conformal dimension $\Delta = 3$. By varying the action of the gravity side with respect to the unknown functions $A(v,r)$, $B(v,r)$, $\Sigma(v,r)$ and $\phi(v,r)$,

one obtains the equations of motion which can be written as follows

$$0 = \Sigma\partial_r(\dot{\Sigma}) + 2\dot{\Sigma}\partial_r\Sigma - 2\Sigma^2 + \frac{1}{12}m^2\phi^2\Sigma^2, \tag{2a}$$

$$0 = 2\partial_r(\dot{\phi}) + \frac{3\partial_r\Sigma}{\Sigma}\dot{\phi} + \frac{3\partial_r\phi}{\Sigma}\dot{\Sigma} - m^2\phi, \tag{2b}$$

$$0 = 2\partial_r(\dot{B}) + \frac{3\partial_r\Sigma}{\Sigma}\dot{B} + \frac{3\dot{\Sigma}}{\Sigma}\partial_r B, \tag{2c}$$

$$0 = \partial_r^2 A - \frac{12}{\Sigma^2}\dot{\Sigma}\partial_r\Sigma + 3\dot{B}\partial_r B + 4 + \dot{\phi}\partial_r\phi - \frac{1}{6}m^2\phi^2, \tag{2d}$$

$$0 = \ddot{\Sigma} - \frac{1}{2}\partial_r A\dot{\Sigma} + \frac{1}{6}\Sigma(3\dot{B}^2 + \dot{\phi}^2), \tag{2e}$$

$$0 = \partial_r^2\Sigma + \frac{1}{6}\Sigma\left(3(\partial_r B)^2 + (\partial_r\phi)^2\right), \tag{2f}$$

where $\dot{h} \equiv \partial_v h + \frac{1}{2}A\partial_r h$ denotes derivative of any function $h(v,r)$ along the radial outgoing null geodesics.

To solve this set of equations, we need to start from an appropriate initial configuration which involves two functions for $B(0,r)$ and $\phi(0,r)$ plus the value of the energy density. The field theory would eventually approach an anisotropic and conformal plasma. Also, we should impose convenient conditions at the boundary, i.e. $r \to \infty$. The bulk metric should approach that of the field theory, which is the 4-dimensional Minkowsky metric and the source of the scalar field is considered to be zero. Having the functions $B(v,r)$ and $\phi(v,r)$ at any time v, we can solve the Eqs. (2) one by one, each one as an ordinary differential equation of r, with the aid of the pseudo-spectral method. Then using an adequate method such as Runge-Kutta we can proceed to the next time step $v + \delta v$. In most cases we choose the following Gaussian profile with tractable parameters $\mathcal{A}$ and β controlling the amplitude and the position of the pulse, respectively

$$f(0,r) = \mathcal{A}\frac{\mathcal{E}}{r^4}\ e^{-150r_h^2\left(\frac{1}{r}-\frac{\beta}{r_h}\right)}. \tag{3}$$

Here $\mathcal{E}$ denotes the energy density and $r_h = \left(\frac{4}{3}\mathcal{E}\right)^{1/4}$ is the event horizon of the final static solution.

In order to study the thermalization process in such a background, one can monitor its dynamics by the use of a variety of observables of the field theory. Local probes, such as the expectation value of the energy-momentum tensor and the scalar field responce, provide valuable information about how the system makes progress towards equilibration. However, by being sensitive to the form of the geometry in the deep IR, nonlocal observables are able to give much more insight into the problem. In what follows, we study the evolution of the two-point correlation function of a local gauge-invariant operator as a nonlocal probe in this background. Next section is devoted to the calculation of this correlation function.

3 Two-point correlation function

We want to calculate the equal-time two-point function for a local scalar operator $\mathcal{O}(t,\mathbf{x})$ of conformal dimension Δ in the aforementioned time-dependent background. For quantum field theories with dimensions higher than two, there is no known technique to calculate the two-point function, analytically. Thus, we have to resort to approximate and/or numerical schemes, specially when we are dealing with non-equilibrium backgrounds. Under special circumstances, we can evaluate it using AdS/CFT correspondence, which relates the two-point function to a path integral including the proper lengths of all possible paths connecting the points $(t,\mathbf{x})$ and $(t,\mathbf{x}')$ at the boundary. For space-like trajectories and large conformal dimension $\Delta \gg 1$ the so-called geodesic approximation can be applied to obtain the following relation for the equal-time two-point function [33, 34]

$$\langle\mathcal{O}(t,\mathbf{x})\mathcal{O}(t,\mathbf{x}')\rangle \approx \sum_{\text{geodesics}} e^{-\Delta\mathcal{L}}, \tag{4}$$

where $\mathcal{L}$ is the real length of the space-like geodesics connecting the boundary points.

This geometrical description explains why the two-point function and other nonlocal probes provide more information than local probes about the evolution of out-of-equilibrium systems. For small enough separations of the boundary points the associated geodesic does not penetrate very much into the bulk and therefore it will thermalize very fast. As we enlarge the separation of the points, the geodesic will penetrate deeper into the bulk and the thermalization of the two points occurs later. This leads us to the conclusion that the ultraviolet degrees of freedom thermalizes first.

3.1 Numerical calculation of the geodesic length

Now, we describe the strategy we use to calculate the length of the space-like geodesics between the two equal-time points $(t_0, -l/2)$ and $(t_0, l/2)$ [26, 27, 32]. These two points can be separated either in the longitudinal direction x_L or in one of the transverse directions $\mathbf{x}_T$ which are the same due to the rotational symmetry in the transverse plane. We take the coordinate of the separation of the points as the parameter of the geodesic between the points and for brevity of notation we denote it simply as x. Therefore, the geodesic will be obtained by determining the functions $v(x)$ and $r(x)$. The following boundary conditions should be fulfilled by these functions

$$r(-l/2) = r(l/2) = r_0,\ v(-l/2) = v(l/2) = t_0, \tag{5}$$

where r_0 is a bulk cut-off close to the boundary. Also, since $v(x)$ and $r(x)$ are symmetric under reflection $x \to -x$, they satisfy the following conditions at the midpoint $x = 0$

$$r'(0) = v'(0) = 0,\ r(0) = r_*,\ v(0) = v_*, \tag{6}$$

The geodesic length between two points on the boundary is obtained by extremizing the length of the curves connecting those two points, which is defined as follows for the bulk metric (1)

$$\mathcal{L} = \int dx \left[-A(v,r)v'(x)^2 + 2v'(x)r'(x) + \tilde{\Sigma}(v,r) \right]^{1/2}, \tag{7}$$

where $\tilde{\Sigma}(v,r) \equiv \Sigma(v,r)^2 e^{B(v,r)}$. We can interpret the integrand of this equation as a Lagrangian and since it is not dependent explicitly on x, there exists a conserved quantity which can be expressed as

$$\tilde{\Sigma}(v_*, r_*)^{1/2} = \frac{\tilde{\Sigma}(v,r)}{\left[-A(v,r)v'(x)^2 + 2v'(x)r'(x) + \tilde{\Sigma}(v,r) \right]^{1/2}}. \tag{8}$$

The left-hand side has been written using the conditions (6). By inserting this relation into the Euler-Lagrange equations obtained by variation of Eq. (7) we obtain two second order differential equations for $v(x)$ and $r(x)$ as follows

$$\begin{aligned} &A(v,r)v''(x) - r''(x) + \left[\frac{\partial_v \tilde{\Sigma}(v,r)}{\tilde{\Sigma}(v,r)} - A(v,r)\frac{\partial_r \tilde{\Sigma}(v,r)}{\tilde{\Sigma}(v,r)} + \partial_r A(v,r) \right] r'(x)v'(x) \\ &+ \left[\frac{1}{2}\partial_v A(v,r) - A(v,r)\frac{\partial_v \tilde{\Sigma}(v,r)}{\tilde{\Sigma}(v,r)} \right] v'(x)^2 + \frac{\partial_r \tilde{\Sigma}(v,r)}{\tilde{\Sigma}(v,r)} r'(x)^2 + \frac{1}{2}\partial_v \tilde{\Sigma}(v,r) = 0, \end{aligned} \tag{9a}$$

$$v''(x) - \frac{\partial_r \tilde{\Sigma}(v,r)}{\tilde{\Sigma}(v,r)} r'(x)v'(x) + \left[\frac{1}{2}\partial_r A(v,r) - \frac{\partial_v \tilde{\Sigma}(v,r)}{\tilde{\Sigma}(v,r)} \right] v'(x)^2 - \frac{1}{2}\partial_r \tilde{\Sigma}(v,r) = 0. \tag{9b}$$

The functions $v(x)$ and $r(x)$ are determined by solving these equations numerically for given values of v_* and r_*. Substituting the profile of the geodesic into Eq. (7), we can determine the corresponding geodesic length as

$$\mathcal{L} = \int_{-l/2}^{l/2} dx \frac{\tilde{\Sigma}(v,r)}{\sqrt{\tilde{\Sigma}(v_*, r_*)}}. \tag{10}$$

We regularize this expression by subtraction of the same quantity computed in pure AdS and find the regularized geodesic length $\mathcal{L}_{\text{reg}}$.

4 Results and concluding remarks

By solving the differential Eqs. (9) with the relations (6) as initial conditions, we are able to find the length of the geodesic corresponding to each pair of v_* and r_*. We have computed the geodesic length as a function of time for several initial configurations by changing the parameters $\beta_{B,\phi}$ and $\mathcal{A}_{B,\phi}$ appearing in the profile (3) for the anisotropy function and the scalar field. Here we report on some conclusions which can be drawn by comparing different initial configurations.

We first set the notation and give some definitions used in this section. In what follows $L(t)$ is the rescaled geodesic length defined as

$$L(t) = \frac{\mathcal{L}_{\rm reg}(t) - \mathcal{L}^{\rm th}_{\rm reg}}{\mathcal{L}^{\rm th}_{\rm reg}}, \tag{11}$$

where $\mathcal{L}^{\rm th}_{\rm reg}$ is the equilibrium value of the regularized geodesic length. We define the equilibration time of the 2-point function ($t_{\rm L}$) as the time after which $|L(t)|$ is lower than ϵ. Moreover, as defined in [22], the equilibration time of the scalar one-point function ($t_{\rm eq}$) is the time after which $|\mathcal{E}^{3/2}\phi_2(t)| < \epsilon$ and the thermalization time ($t_{\rm th}$) is the time after which the entropy production ends or equivalently the event horizon reaches its equilibrium, and can be determined by $\left|\frac{r_{EH}(t_{\rm th})-\pi T}{\pi T}\right| < \epsilon$ where $r_{EH}(t)$ and T are the event horizon radius and the final temperature of the plasma, respectively. Notice that ϵ is a small number that sets the precision for determining the time-scales and is chosen to be 0.0005 in most of the cases here. The results that are reported below have been checked for different precisions and we found them to be independent of the choice of this number. Furthermore, in all figures the boundary time t has been rescaled in units of the temperature of the final static black hole, i.e. $T = 1/\pi$.

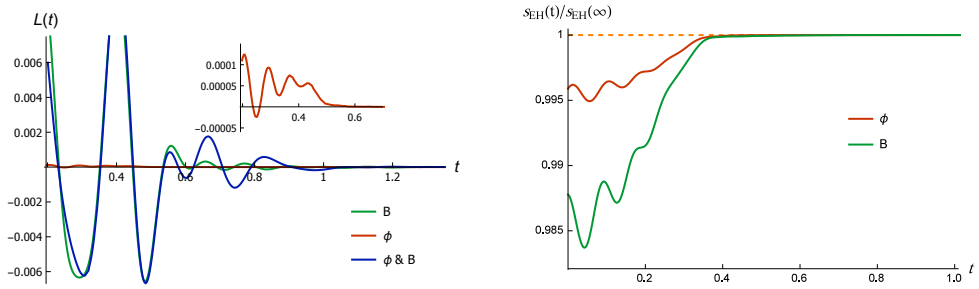

Figure 1: Left graph: geodesic length versus time for the transverse separation $l = 1$ and right graph: the time evolution of the entropy density. Green, red and blue lines are the graphs for the initial configurations with $\phi = 0$, $B = 0$ and the case with both functions present, respectively. The functions are in the form of Eq. (3) with parameters $\beta_B = 1/2$, $\mathcal{A}_B = 6/15$, $\beta_\phi = 1/2$ and $\mathcal{A}_\phi = 6/15$.

In the left panel of Fig. 1 we have presented the rescaled geodesic length for two points separated by $l = 1$ in the transverse direction. Here we consider the evolution of three different initial out-of-equilibrium plasma: anisotropic and conformal plasma ($B(0,r) \neq 0$), isotropic and non-conformal plasma ($\phi(0,r) \neq 0$), and anisotropic and non-conformal plasma (nonzero $B(0,r)$ and $\phi(0,r)$). From the graphs we can see that for an initial configuration with the same values of β and $\mathcal{A}$ for both functions of the scalar field and anisotropy, the equilibration time of $L(t)$ mostly comes from the anisotropy function. As can be seen in Fig. 2, the scalar field has noticeable effects on the evolution of $L(t)$ only if it is chosen to have significantly larger values of β and/or $\mathcal{A}$ as compared to the anisotropy function. These results indicate that the anisotropy function can drive the geometry out of equilibrium much easier than the scalar field, as viewed by the two-point function.

It is interesting to consider the thermalization time for the first two backgrounds. The entropy density versus time for these backgrounds has been shown in the right panel of Fig. 1. It is obvious that the time at which the entropy production ends for these systems is very close. By choosing ϵ to be 0.0001, the ratio of $t_{\rm th}$ for the second system with respect to the first one is obtained about 0.85, while the same ratio for $t_{\rm L}$ is about 0.27. This means that from the viewpoint of the two-point function, as a nonlocal probe, the first system is much farther away from equilibrium than the second one,

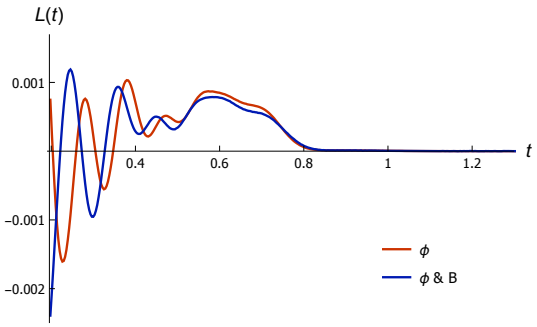

Figure 2: Geodesic length versus time for the transverse separation $l = 1$. Red and blue lines are the graphs for the initial configurations with $B = 0$ and both functions present, respectively. The parameters of the functions are $\beta_B = 1/6$, $\mathcal{A}_B = 2/15$, $\beta_\phi = 5/6$ and $\mathcal{A}_\phi = 10/15$.

while taking the entropy density as an observable which is also sensitive to lower energy scales in the field theory (and equivalently sensitive to the bulk geometry in the deep IR) there is no considerable difference between these systems. The large difference between the equilibration time of the two-point function on top of these systems may refer to the result we found in [22], which indicates that the scalar field acts as a probe to the AdS-black hole after the event horizon reaches its equilibrium.

Now, we want to compare the time evolution of two different observables: the normalizable mode of the scalar field ϕ, which corresponds to the one-point function of the dual operator in the field theory and therefore is a local observable, and the length of the geodesic connecting two points on the boundary, which gives the correlation between these points in the field theory and hence is a nonlocal probe with a nonzero size. Choosing the initial anisotropy function and scalar field in the form of the profile (3) with parameters $\beta_B = 1/4$, $\mathcal{A}_B = 2/15$, $\beta_\phi = 1/6$ and $\mathcal{A}_\phi = 2/15$, we have let the system to evolve and approach its equilibrium. Then, on top of this time-dependent background, we have calculated the equilibration time of the correlation function between two points on the boundary, and indicated the results for different separations l in Fig. 3 by some points. From this figure the dependence of the equilibration time on the size of the probe is evident, as is known in the literature (for example [26]), i.e. wider probes thermalize later than narrower ones. We have also shown the

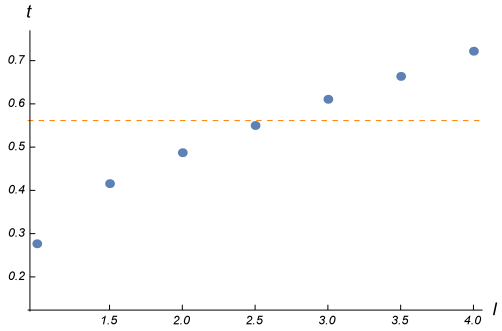

Figure 3: Equilibration time of the 2-point function versus the separation l, for an initial configuration in which both the anisotropy function and scalar field are in the form of the profile (3) with parameters $\beta_B = 1/4$, $\mathcal{A}_B = 2/15$, $\beta_\phi = 1/6$ and $\mathcal{A}_\phi = 2/15$. The dashed line indicates the equilibration time of the response of the scalar field.

equilibration time of the scalar field response in Fig. 3 by a horizontal dashed line. It is important to notice that not for all values of l the two-point function equilibrates after the one-point function of the scalar field.

From Fig. 3 we see that $t_{\rm L} < t_{\rm eq}$ for the correlation between two points with the transverse separation $l = 1$. The time evolution of the two observables for $l = 1$ has been depicted in the left panel of Fig. 4. In the right panel of this figure the evolution of the two-point function for another initial configuration

with parameters $\beta_B = 5/6$, $\mathcal{A}_B = 4/15$, $\beta_\phi = 1/6$ and $\mathcal{A}_\phi = 2/15$ has been shown. Although in both cases $l = 1$, it is obvious that in the left graph the two-point function equilibrates before the one-point function, while in the right graph the local operator equilibrates first. One can draw the conclusion that by changing the initial configuration the ordering of the equilibration of local and nonlocal probes can change. Therefore, the ordering of the equilibration times can be determined only after the exact form of the initial configuration is known. There is an important issue we should address here. If there exists only one source for driving the system out of equilibrium, the situation is different. In this case the ordering of the local and nonlocal equilibration times cannot be reversed by just changing the parameters of the initial configuration. For example, suppose that for a chosen out-of-equilibrium system which is isotropic from the beginning and the scalar field is in the form of Eq. (3) with some parameters β_ϕ and $\mathcal{A}_\phi$, $t_{\rm L} < t_{\rm eq}$ for transverse separation $l = 1$. This relation will always hold, no matter how we change the parameters of the initial profile.

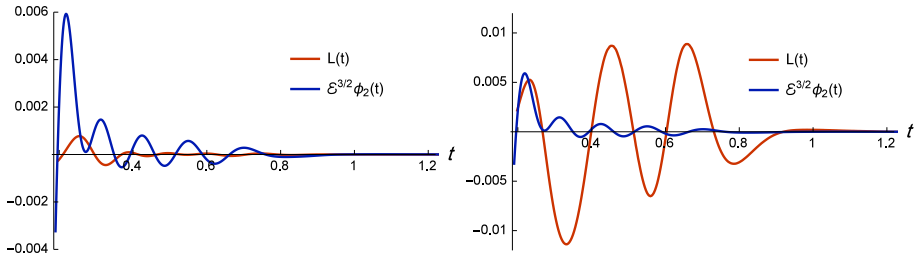

Figure 4: The parameters of the initial functions in the left panel are $\beta_B = 1/4$, $\mathcal{A}_B = 2/15$, $\beta_\phi = 1/6$ and $\mathcal{A}_\phi = 2/15$, and in the right panel are $\beta_B = 5/6$, $\mathcal{A}_B = 4/15$, $\beta_\phi = 1/6$ and $\mathcal{A}_\phi = 2/15$. Red and blue lines are the rescaled geodesic length and the scalar field response, in both graphs.

Another interesting observation from Fig. 3 is the linear increase of the two-point function equilibration time $t_{\rm L}$ for large enough values of the size l. This feature has also been observed in other systems [29, 32]. By checking other initial conditions, we found that this behavior is independent of the initial configuration that we start with. Moreover, we found that $t_{\rm L}$ increases linearly in time with approximately the same slope for different initial configurations. This behavior can be observed in Fig. 5 where we have shown the results for two cases. Blue dots are the results obtained for the same configuration as the one drawn in Fig. 3 in which both the anisotropy function and scalar field have the form of the profile (3) with parameters $\beta_B = 1/4$, $\mathcal{A}_B = 2/15$, $\beta_\phi = 1/6$ and $\mathcal{A}_\phi = 2/15$. Red dots show the equilibration times for a completely different initial configuration in which no scalar field is present and the anisotropy function is in the form of $B(0, r) = 2\mathcal{E}r^{-4}$. This feature seems to emerge due to the invariance of the initial conditions under the translational symmetry. Notice that all the initial configurations employed here, are independent of the spatial coordinates of the boundary, i.e. x_L and $\mathbf{x}_T$. It would be interesting to consider this problem in nontrivial cases where such an invariance is absent, for example in the case of shock wave collisions.

The evolution of the tip of the geodesics located at $x = 0$ is displayed in Fig. 6 for different transverse separations. In this figure we also show the position of the event horizon as time proceeds. Here the anisotropy function on the initial time slice is chosen to be $B(0, r) = \frac{8}{3}\mathcal{E}r^{-4}$ while the scalar field has been turned off from the beginning. As can be seen, for the initial configuration chosen here, the event horizon reaches its equilibrium very early at a time much less than 0.2. However, the two-point functions approach their equilibrium much later. It is also evident that the time for the equilibration as viewed by these probes, depends on the size of the probe in the field theory and this again supports the idea of faster thermalization at higher energies for strongly-coupled theories. An interesting phenomenon that can be observed from this figure, is that for sufficiently large boundary separations and after enough amount of time the geodesics cross the event horizon, while at early times they are all outside the horizon. At sufficiently late times they all approach their equilibrium values which are outside the event horizon. It would be interesting to check this result for the case of the extremal surfaces dual to the holographic entanglement entropy in the present background and compare it with the surprising result found in [31] for colliding gravitational shock waves. They found

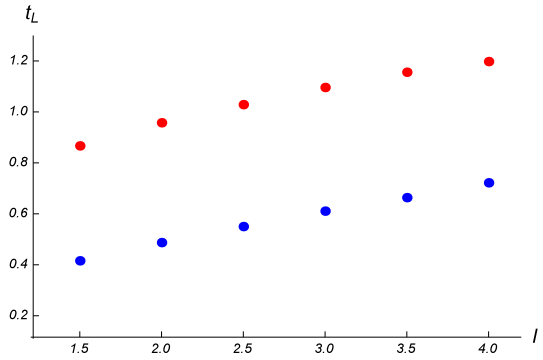

Figure 5: The equilibration time of the two-point function versus the size l shown with the blue and red dots, respectively, for the following initial configurations. In the first case the anisotropy function and scalar field are in the form of the profile (3) with parameters $\beta_B = 1/4$, $\mathcal{A}_B = 2/15$, $\beta_\phi = 1/6$ and $\mathcal{A}_\phi = 2/15$, and in the second one $B(0,r) = 2\mathcal{E}r^{-4}$ and $\phi(0,r) = 0$.

that for larger separations the geodesics can extend behind the apparent horizon, meaning that the two-point correlation functions probe behind the horizon, while they did not found such a conclusion for the entanglement entropy.

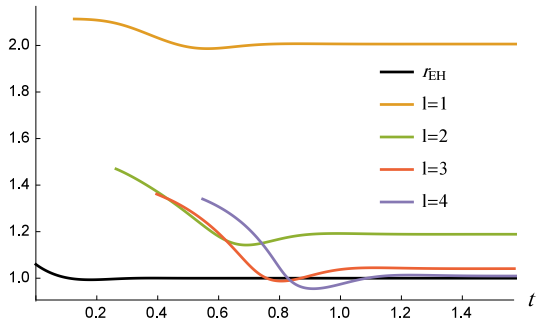

Figure 6: The r position of the tip of various geodesics corresponding to different transverse separations at the boundary along with the r position of the event horizon (the black curve).

Acknowledgement

We thank Michal P. Heller for very useful discussions and also giving lectures at IPM. H. E. would like to thank Wilke van der Schee for fruitful discussions.

References

[1] E. Shuryak, "Why does the quark gluon plasma at RHIC behave as a nearly ideal fluid?," Prog. Part. Nucl. Phys. **53**, 273 (2004) [arXiv:hep-ph/0312227].

[2] E. V. Shuryak, "What RHIC experiments and theory tell us about properties of quark-gluon plasma?," Nucl. Phys. A **750**, 64 (2005) [arXiv:hep-ph/0405066].

[3] U. W. Heinz, "Thermalization at RHIC," AIP Conf. Proc. **739**, 163 (2005) [arXiv:nucl-th/0407067].

[4] J. M. Maldacena, "The large N limit of superconformal field theories and gravity," Adv. Theor. Math. Phys. **2**, 231 (1998) [Int. J. Theor. Phys. **38**, 1113 (1999)] [arXiv:hep-th/9711200].

[5] S. S. Gubser, I. R. Klebanov and A. M. Polyakov, "Gauge theory correlators from non-critical string theory," Phys. Lett. B **428**, 105 (1998) [arXiv:hep-th/9802109].

[6] E. Witten, "Anti-de Sitter space and holography," Adv. Theor. Math. Phys. **2**, 253 (1998) [arXiv:hep-th/9802150].

[7] J. Casalderrey-Solana, H. Liu, D. Mateos, K. Rajagopal and U. A. Wiedemann, "Gauge/string duality, hot QCD and heavy ion collisions," [arXiv:1101.0618 [hep-th]].

[8] Y. V. Kovchegov and A. Taliotis, "Early time dynamics in heavy ion collisions from AdS/CFT correspondence," Phys. Rev. C **76**, 014905 (2007) [arXiv:0705.1234 [hep-ph]].

[9] S. Bhattacharyya and S. Minwalla, "Weak field black hole formation in asymptotically AdS spacetimes," JHEP **0909**, 034 (2009) [arXiv:0904.0464 [hep-th]].

[10] P. M. Chesler and L. G. Yaffe, "Horizon formation and far-from-equilibrium isotropization in supersymmetric Yang-Mills plasma," Phys. Rev. Lett. **102**, 211601 (2009) [arXiv:0812.2053 [hep-th]].

[11] P. M. Chesler and L. G. Yaffe, "Boost invariant flow, black hole formation, and far-from-equilibrium dynamics in N = 4 supersymmetric Yang-Mills theory," Phys. Rev. D **82**, 026006 (2010) [arXiv:0906.4426 [hep-th]].

[12] T. Albash and C. V. Johnson, "Evolution of holographic entanglement entropy after thermal and electromagnetic quenches," New J. Phys. **13**, 045017 (2011) [arXiv:1008.3027 [hep-th]].

[13] J. Aparicio and E. Lopez, "Evolution of two-point functions from holography," JHEP **12**, 082 (2011) [arXiv:1109.3571 [hep-th]].

[14] M. P. Heller, D. Mateos, W. van der Schee and D. Trancanelli, "Strong coupling isotropization of non-Abelian plasmas simplified," Phys. Rev. Lett. **108**, 191601 (2012) [arXiv:1202.0981 [hep-th]].

[15] R. Auzzi, S. Elitzur, S. B. Gudnason and E. Rabinovici, "On periodically driven AdS/CFT," JHEP **1311**, 016 (2013) [arXiv:1308.2132 [hep-th]].

[16] M. P. Heller, D. Mateos, W. van der Schee and M. Triana, "Holographic isotropization linearized," JHEP **1309**, 026 (2013) [arXiv:1304.5172 [hep-th]].

[17] E. Caceres, A. Kundu, J. F. Pedraza and W. Tangarife, "Strong subadditivity, null energy condition and charged black holes," JHEP **01**, 084 (2014) [arXiv:1304.3398 [hep-th]].

[18] H. Liu and S. J. Suh, "Entanglement tsunami: Universal scaling in holographic thermalization," Phys. Rev. Lett. **112**, 011601 (2014) [arXiv:1305.7244 [hep-th]].

[19] P. M. Chesler and L. G. Yaffe, "Numerical solution of gravitational dynamics in asymptotically anti-de Sitter spacetimes," JHEP **1407**, 086 (2014) [arXiv:1309.1439 [hep-th]].

[20] T. Ishii, S. Kinoshita, K. Murata and N. Tanahashi, "Dynamical meson melting in holography," JHEP **1404**, 099 (2014) [arXiv:1401.5106 [hep-th]].

[21] M. Ali-Akbari, F. Charmchi, A. Davody, H. Ebrahim and L. Shahkarami, "Evolution of Wilson loop in time-dependent N=4 super Yang-Mills plasma," Phys. Rev. D **93**, 086005 (2016) [arXiv:1510.00212 [hep-th]].

[22] M. Ali-Akbari, F. Charmchi, H. Ebrahim and L. Shahkarami, "Various time-scales of relaxation," Phys. Rev. D **94**, 046008 (2016) [arXiv:1602.07903 [hep-th]].

[23] D. Kaviani, "D7-brane dynamics and thermalization in the Kuperstein-Sonnenschein model," [arXiv:1608.02380 [hep-th]].

[24] M. Atashi, K. B. Fadafan and G. Jafari, "Linearized holographic isotropization at finite coupling," [arXiv:1611.09295 [hep-th]].

[25] V. Balasubramanian, A. Bernamonti, J. de Boer, N. Copland, B. Craps, E. Keski-Vakkuri, B. Mller, A. Schfer, M. Shigemori and W. Staessens, "Thermalization of strongly coupled field theories," Phys. Rev. Lett. **106**, 191601 (2011) [arXiv:1012.4753 [hep-th]].

[26] V. Balasubramanian, A. Bernamonti, J. de Boer, N. B. Copland, B. Craps, E. Keski-Vakkuri, B. Mller, A. Schfer, M. Shigemori and W. Staessens, "Holographic thermalization," Phys. Rev. D **84**, 026010 (2011) [arXiv:1103.2683 [hep-th]].

[27] D. Galante and M. Schvellinger, "Thermalization with a chemical potential from AdS spaces," JHEP **1207**, 096 (2012) [arXiv:1205.1548 [hep-th]].

[28] J. F. Pedraza, "Evolution of nonlocal observables in an expanding boost-invariant plasma," Phys. Rev. D **90**, 046010 (2014) [arXiv:1405.1724 [hep-th]].

[29] A. Buchel, R. C. Myers and A. van Niekerk, "Nonlocal probes of thermalization in holographic quenches with spectral methods," JHEP **02**, 017 (2015) [JHEP **07**, 137 (2015)] [arXiv:1410.6201 [hep-th]].

[30] C. Ecker, D. Grumiller and S. A. Stricker, "Evolution of holographic entanglement entropy in an anisotropic system," JHEP **07**, 146 (2015) [arXiv:1506.02658 [hep-th]].

[31] C. Ecker, D. Grumiller, P. Stanzer, S. A. Stricker and W. van der Schee, "Exploring nonlocal observables in shock wave collisions," JHEP **1611**, 054 (2016) [arXiv:1609.03676 [hep-th]].

[32] L. Bellantuono, P. Colangelo, F. de Fazio, F. Giannuzzi and S. Nicotri, "Role of nonlocal probes of thermalization for a strongly interacting non-Abelian plasma," Phys. Rev. D **94**, 025005 (2016) [arXiv:1603.08849 [hep-ph]].

[33] V. Balasubramanian and S. F. Ross, "Holographic particle detection," Phys. Rev. D **61**, 044007 (2000) [arXiv:hep-th/9906226].

[34] G. Festuccia and H. Liu, "Excursions beyond the horizon: Black hole singularities in Yang-Mills theories (I)," JHEP **04**, 044 (2006) [arXiv:hep-th/0506202].